Journal of Ocean University of China (Oceanic and Coastal Sea Research)
ISSN 1672-5182, October 30, 2007, Vol.6, No.4, pp.349-354
http://www.ouc.edu.cn/xbywb/
E-mail:xbywb@ouc.edu.cn

Study of the Corrosion Resistance of Electroless Ni-P Deposits in a Sodium Chloride Medium

GAO Rongjie[1)], DU Min[2),*], SUN Xiaoxia[2)], and PU Yanli[2)]

1) *Institute of Material Science and Engineering*, *Ocean University of China*, *Qingdao* 266100, *P. R. China*
2) *College of Chemistry and Chemical Engineering*, *Ocean University of China*, *Qingdao* 266100, *P. R. China*

(Received March 23, 2006; accepted May 16, 2007)

Abstract The corrosion resistance of electroless Ni-P deposits with phosphorous contents from 12% to 14% in sodium chloride solutions was studied. The deposits were immersed in 3.5% NaCl solutions for 29 d to obtain the electrochemical parameters and were examined in a standard salt spray test for 15 d respectively. The corrosion resistance of the deposits was studied by potentio-dynamic scan, electrochemical impedance spectroscopy (EIS), X-ray diffraction (XRD) and cold-field emission scanning electron microscopy (FE-SEM) equipped with an energy dispersive X-ray detector (EDX). The patterns of XRD and the results of FE-SEM showed that the prepared deposits were amorphous. But after a 15 d standard salt spray test, a few pinholes appeared on the surface of the deposit and the weight content of phosphorus on the surface of the deposit was higher (which was beneficial to the formation of the passivation films) than that before the standard salt spray test when the nickel content was lower because the dissolved weight of nickel was greater than that of phosphorus. The results from potentio-dynamic scan and EIS showed that passivation films formed on the Ni-P deposit after immersion in the NaCl solutions, which decreased the corrosion rate of Ni-P samples. The results of this work show their potential applications in marine corrosion.

Key words electroless Ni-P deposit; corrosion resistance; passivation film; amorphous

DOI 10.1007/s11802-007-0349-2

1 Introduction

Owing to the characteristics of Ni-P deposits, *e.g.*, anticorrosion, wear resistance, paramagnetism, high hardness and the electro-catalytic activity of hydrogen evolution (Hajdu, 1996; Han *et al.*, 1996; Feldstein and Thomas, 1980; Donald *et al.*, 1984; Mallory and Lioyd, 1985; Taloat *et al.*, 1993), Ni-P deposits are being widely used in various fields.

Ni-P and Ni-M-P deposits were found to be good anti-corrosive coatings in several media (Sun *et al.*, 1992; Yang *et al.*, 2000; Hou, 2000; David and Brown, 1997; Xu and Wei, 2000). The formation of a passive film on Ni-P coatings was also found to be easier than that on a pure nickel coating in acidic environments due to the presence of phosphorous alloyed with nickel (Lin and Lai, 1989). In addition, an enrichment of phosphorus on the surface of Ni-P coatings has been observed in potential regions where hydrogen evolution and passivation occur. Recently, much attention has been devoted to the anti-corrosive behavior of Ni-P coatings, including the content and distribution of phosphorous as well as its surface morphology and structure in corrosive environments (Lin and Lai, 1989). All these studies show that the phosphorus content of a Ni-P coating is expected to play an important role in the passivity.

In this work, in order to use electroless Ni-P deposits successfully in the marine environment, the corrosion resistance of Ni-P deposits with phosphorous contents from 12% to 14% was studied in 3.5% NaCl (the same infra) solutions by potentio-dynamic scan, electrochemical impedance spectroscopy (EIS), X-ray diffraction (XRD) and cold-field emission scanning electron microscopy (FE-SEM) equipped with an energy dispersive X-ray detector (EDX).

2 Experiments

The Ni-P deposits were plated onto 2 cm×2 cm Q235B carbon steel plates. The components of Q235B are listed in Table 1. These Q235B plates were first polished by using 800 grit sand papers, degreased with ethanol or lye, rinsed with pure water, and then derusted with 6 mol L^{-1} HCl for 10 min and activated in mixed acids at 140℃ for 10 s, and finally rinsed with pure water. After being cleaned, the plates were appended in the Ni-P baths with a loadage of 1 L dm^{-2} which was heated by a water bath.

The Ni-P baths contained 18−19 g L^{-1} $NiSO_4 \cdot 6H_2O$,

* Corresponding author. Tel: 0086-532-66781637
E-mail: ssdm99@ouc.edu.cn

24 g L^{-1} $NaH_2PO_2 \cdot H_2O$, 16−21 g L^{-1} malic acid, 18−23 g L^{-1} butyric acid and 8−24 mg L^{-1} stabilizing agent with a pH value adjusted with 0.5 mol L^{-1} ammonia and 0.5 mol L^{-1} H_2SO_4 to 4.8−5.0. Ni-P deposits of about 24 μm thickness were obtained after plating for 2 h at 85℃−90℃. For electrochemical studies, the electrodes were covered with epoxy resin leaving an exposed area of 1.0 cm^2.

Table 1 Components of Q235B carbon steel

Component	C	Si	Mn	P	S	Fe
Content (%)	0.22	0.05	0.48	0.012	0.022	remainder

The deposits were examined by standard salt spray test for 15 d, the solution being 5% NaCl and the pH being 6.5−7.2. The samples with deposits were placed on a bracket in the middle of the experiment chest and the salt fog settled freely on the surface of the deposits. The temperature in the chest was 35℃±1℃ and the sedimentation rate was 1−2 mL $(80\ cm^2)^{-1}\ h^{-1}$.

The corrosion resistance of the Ni-P deposits was also measured by electrochemical methods such as EIS and potentio-dynamic polarization on the impedance spectrum analyzer (IM6e, ZAHNER, Germany) at E_{ocp} with 5 mV AC amplitude in (3.5%) NaCl solutions, where E_{ocp} was the open circuit potential of the deposits in NaCl solutions and it ranged from –0.4 V to –0.25V (vs. SCE, the same infra). The AC frequencies ranged from 100 kHz to 10 mHz. The scan rate was 20 mV min^{-1} during the potentio-dynamic polarization. In the electrochemical measurements, a saturated calomel electrode (SCE) was used as the reference electrode and a piece of platinum gauze was employed as the counter electrode. A Luggin capillary, whose tip was set at a distance of 1−2 mm from the surface of the working electrode, was used to minimize errors due to IR drop in the electrolytes.

The surface configuration and the composition of the Ni-P deposits were examined by X-ray diffraction (XRD, $D_{max}/\gamma\beta$, Rigaku, Japan) and cold-filed emission scanning electron microscope (FE-SEM, JSM-6700F, Japan) equipped with an energy dispersive X-ray detector (EDX, INCA Energy, England).

3 Results and Discussion

3.1 The Standard Salt Spray Test

Six samples were prepared by the procedure described above for the standard salt spray test. After the Ni-P deposits were corroded in the standard salt spray test, the corrosion rates were obtained and are listed in Table 2. The average annual corrosion rates of all the samples were approximately 0.023 mm per year. An optical micrograph of the corroded Ni-P deposit surface is presented in Fig.1. It can be seen that apart from a couple of pinholes the corrosion is generally uniform.

Table 2 Corrosion rates of the deposits in standard salt spray test

Number	1	2	3	4	5	6
Corrosion rate (g $m^{-2}\ d^{-1}$)	0.3638	0.4228	0.3702	0.4156	0.4421	0.5395
Average corrosion rate (g $m^{-2}\ d^{-1}$)			0.4257			
Average Annual corrosion rate (mm $year^{-1}$)			0.0233			

Fig.1 An optical micrograph of Ni-P deposit surface after standard salt spray test.

3.2 The Polarization Curves in NaCl Solutions

The polarization curves of Ni-P deposits measured in 3.5% NaCl solutions after 0.5 h, 2 d, 6 d, 13 d and 29 d are shown in Fig.2.

There was a passive phenomenon, though not obvious, on the Ni-P deposits after they were immersed in the solutions for 0.5 h. When the electrode potential increased from –400 mV to –200 mV, the current density ascended sharply, which was due to the slight anode dissolution in this period. When the potential increased from –200 mV to 300 mV, the current density increased slightly, implying the entering of the Ni-P deposits into the passive period.

It can be seen that the passive phenomenon was increasingly obvious with the increase of immersion time in NaCl solutions. After immersion periods of 2, 6, 13 and 29 d, the open circuit potential of the tested samples drifted to –0.3 V from –0.4 V, indicating that the Ni-P deposits had positive effects on reducing the corrosion rate in the active corrosion region. The sequence of the deposits with respect to decrease in corrosion currents for the same potential from –0.05 V to 0.15 V was: 2 d < 6 d <

13 d < 29 d. And passive phenomena were found in these deposits. But with the prolonging of the time in the NaCl solutions, E_b decreased and the passivation period became increasingly narrow, indicating that the porosity resistance of the deposits declined.

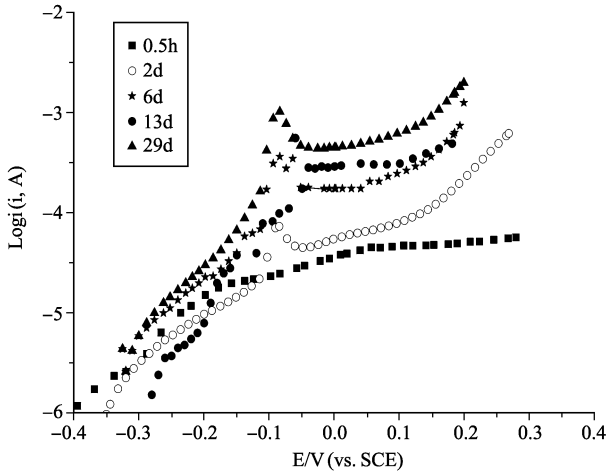

Fig.2 Polarization data of the deposits in3.5% NaCl solutions.

3.3 Electrochemical Impedance Spectroscopy (EIS) Study of Ni-P Deposits in NaCl Solution

The anticorrosive ability of Ni-P deposits during the experiment was investigated by using the EIS data in Fig.3. Two types of data distribution were found in using electrochemical impedance spectroscopy (EIS) techniques. One was for the deposit immersed in NaCl solution for 0.5h; the other was for the deposits immersed for 2, 6, 13 and 29 d. The equivalent circuit for the first type is shown in Fig.4 with the corresponding data presented

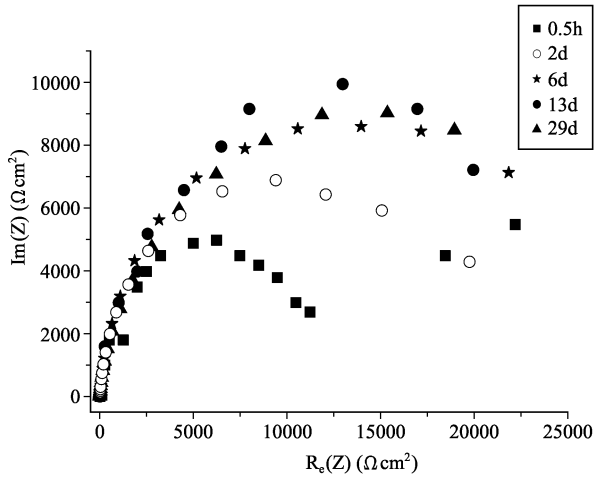

Fig.3 EIS data of Ni–P deposits in 3.5% NaCl solutions.

in Table 3. There was a high diffusion resistance when the deposit was immersed in NaCl solution for 0.5 h. This was because a passivation film had formed on the surface of the deposit and it was difficult for the solution to penetrate the passivation film, which was consistent with the behavior of data in Fig.2.

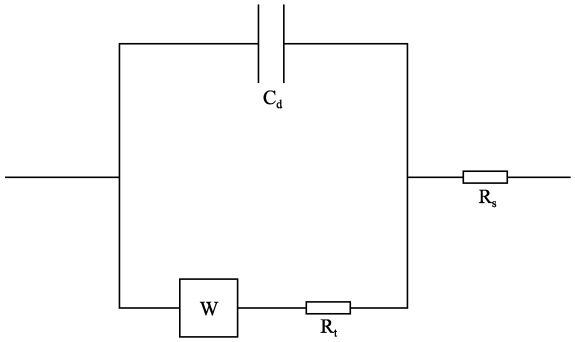

Fig.4 Equivalent model of the deposits after immersion in 3.5% NaCl solutions for 0.5 h. C_d: capacitance of the deposit/solution; R_s: solution resistance; W: Warburg resistance; R_t: charge transfer resistance.

Table 3 Electrochemical parameters of the model in Fig.4

R_t (kΩ cm^2)	C_d (μF cm^{-2})	W (DW)	R_s (Ω cm^2)
8.46	87.09	680.71	0.65

Fig.5 is the equivalent circuit of Ni-P after being immersed in NaCl solution for 2, 6, 13 and 29 d and the related data are shown in Table 4. After the deposits were immersed in NaCl solution for 2 d, two time constants appeared in the impedance spectra. The high-frequency time constant reflected the characteristics of the charge-transfer resistance R_t of the deposits and the low-frequency time constant reflected the characteristics of the resistance of the passivation films R_f on the deposits. Then for the polarization resistance R_p we have $R_p = R_t + R_f$. After the deposits were immersed in NaCl solution for 6, 13 and 29 d, the polarization resistance (R_p) fluctuated in the range of 20 to 22 kΩ cm^2. With the increase of

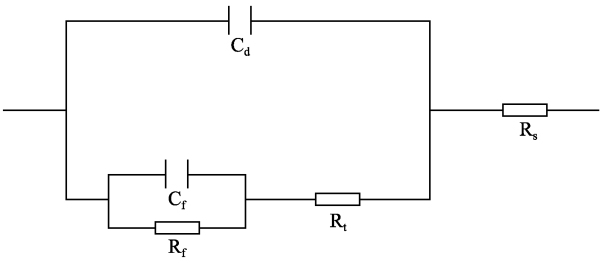

Fig.5 Equivalent model of the deposits after being immersed in 3.5% NaCl for over 2 d. C_f: capacitance of the passivation film/solution; R_s: solution resistance; C_d: capacitance of the deposit/solution; R_f: resistance of the film; R_t : charge transfer resistance.

immersion time in NaCl solution, the charge transfer resistance (R_t) decreased from 16.57 to 6.18 kΩ cm^2 and C_f decreased from 36.01 to 0.14 μF cm^{-2}, which indicated that the pinholes began to appear on the deposits when the immersion time reached 6 d. Correspondingly, the film resistance (R_f) on the Ni-P deposit increased from 0.03 to 15.44 kΩ cm^2 and C_d increased from 92.46 to 99.32 μF cm^{-2} when the immersion time reached 6 d, which indicated the formation of the passivation film. But after 6 d,

changes of the film resistance and the charge transfer resistance, which were about 16 and 6 $k\Omega cm^2$ respectively, were not obvious, implying that the passivation film was stable after 6 d.

Table 4 Electrochemical parameters of the model in Fig.5

Time (d)	EIS Data				
	R_f ($k\Omega \cdot cm^2$)	R_t ($k\Omega \cdot cm^2$)	R_s ($\Omega \cdot cm^2$)	C_f ($\mu F \cdot cm^{-2}$)	C_d ($\mu F \cdot cm^{-2}$)
2d	0.03	16.57	0.74	36.01	92.46
6d	15.44	6.18	0.92	0.14	99.32
13d	17.88	5.77	1.51	0.17	101.48
29d	16.99	5.71	1.22	0.22	100.51

3.4 Surfaces and Structures of the Ni-P Deposits Before and After the Standard Salt Spray Test

The XRD patterns of the Ni-P deposits were shown in Fig.6, where (Fig.6a) only one broad peak with a weak intensity appeared at about $2\theta=45^\circ$ implying that the deposits were amorphous. The intensity of the Ni-P deposits increased remarkably after the standard salt spray test, which may indicate slight crystallization of some parts of the Ni-P deposits. Two sharp diffraction peaks around $2\theta=45^\circ$, possibly due to the oxide of the nickel or Ni_yP_x, such as Ni_2O_5 ($2\theta=43.8^\circ$), Ni_3P ($2\theta=43.8^\circ$) or Ni_2O_3 ($2\theta=45.0^\circ$), appeared in the XRD patterns after the standard salt spray test, as shown in Fig.6(b). This deduction was proven by the result that there was about 5.33% oxygen on the Ni-P deposits after the salt spray test. The Ni-P deposits are composed of tiny crystals which possibly fill the interstices of the amorphous Ni-P deposits (Niu *et al.*, 2003).

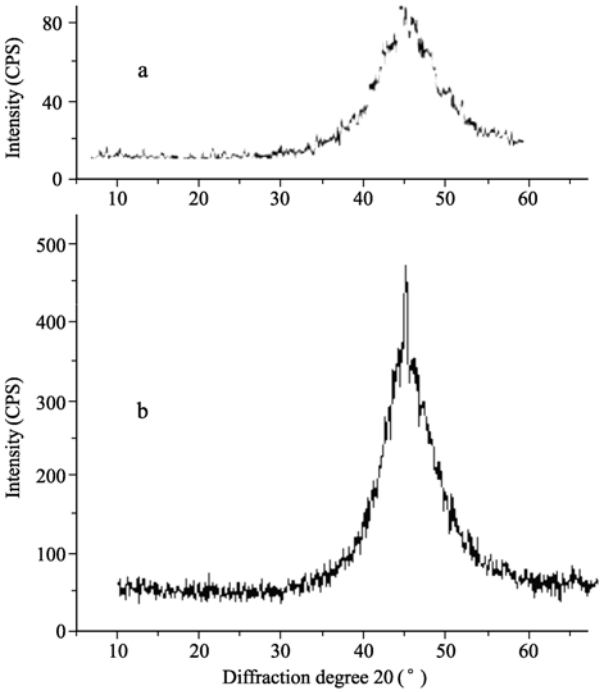

Fig.6 XRD of the Ni-P deposits before and after corrosion. a: prepared deposits. b: after the standard salt spray test.

The surfaces and the structures of the Ni-P deposits before and after the standard salt spray test are presented in Figs.7 and 8 respectively.

From Fig.7 and Table 5, we see that the prepared Ni-P film had only two elements, Ni (86.03%) and P (13.97%), and it belonged to deposits with high-content phosphorus and had no obvious pinholes.

Fig.8 shows that there are a few pinholes, which mainly exist among the spherules, in the deposit after the standard salt spray test. From Table 5 we see that the weight content of Ni on the surface decreased from 86.03% to 71.13% after the standard salt spray test, which indicated that the nickel on the surface dissolved in the NaCl solutions. However, the weight content of P increased from 13.97% to 15.51%, while that of nickel decreased and the atomic contents of Ni and P were all less than those before the standard salt spray test. This indicated that the P had only dissolved in part when the Ni had dissolved, for the structure of the deposit was not uniform. And the dissolved weight of nickel was greater than that of P. There were elements Na and Cl on the surface because the sample was not sufficiently cleaned after the salt spray test. In addition, the element Fe was detected and there was about 5.33% oxygen on the surface.

Diegle *et al.* (1988) considered that the phosphorus in the Ni-P deposits could be oxygenated to form passivation films in corrosive media. The passivation films could reduce the corrosion rate of the deposits. From Fig.8, we see that oxygen was present in the deposit. It could be deduced that part of the nickel was dissolved and part of it was oxidized to form nickel oxides, and that the phosphorus were oxidized to form phosphides. So the weight content of P on the surface was higher than that in the prepared deposits while the content of nickel was lower, which was also consistent with the energy spectrum result in Table 5.

In corrosive media, the corrosion rate of the deposits is determined by the dissolution of the phosphide films. When the deposits are amorphous, the chemical components and the structure are homogeneous, and then the phosphide films are smooth, so the corrosion rate of the deposits is relatively low. After corrosion, the phosphorus content on the surface of the deposits increases, so the phosphide films are more compact and the dissolution rate becomes lower, decreasing the corrosion rate. These are the reasons why the Ni-P deposits have good anticorrosion property.

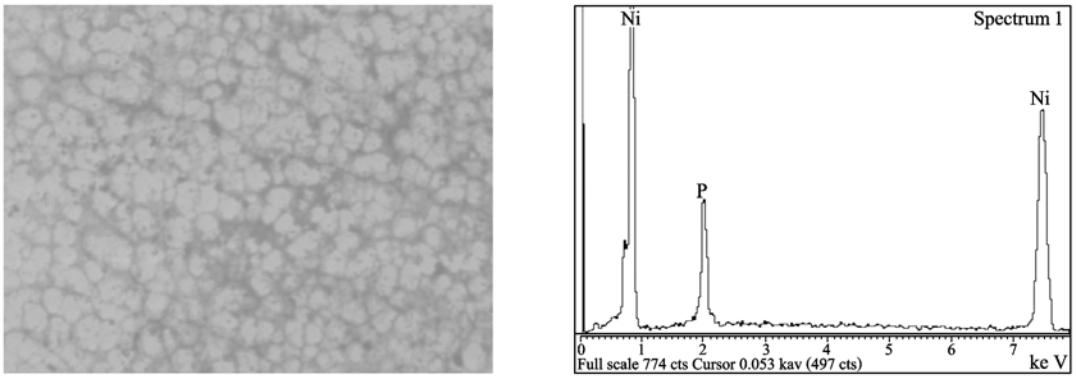

Fig.7 FE-SEM image (left) and energy spectrum (right) of the prepared Ni-P deposits.

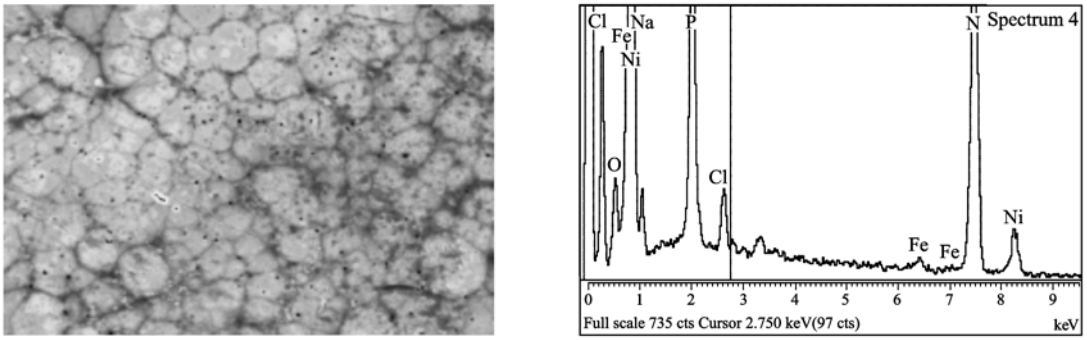

Fig.8 FE-SEM image (left) and energy spectrum (right) of the Ni-P deposits after the salt spray test.

Table 5 Elements of the deposits detected by energy spectrum before and after the standard salt spray test

Before			After		
Element	Weight (%)	Atomic (%)	Element	Weight (%)	Atomic (%)
			O	5.33	14.26
			Na	4.74	8.83
P	13.97	23.54	P	15.51	21.43
			Cl	2.49	3.01
			Fe	0.80	0.61
Ni	86.03	76.46	Ni	71.13	51.86
Totals	100.0		Totals	100.00	

4 Conclusion

Both the polarization and the EIS data could be divided into two kinds, one corresponding to immersion time 0.5 h in NaCl solutions and the other corresponding to immersion time 2, 6, 13 and 29 d. At the beginning of immersion, a passivation film started to form on the deposit, but it was not integrated. The passivation phenomenon became increasingly obvious as the immersion time increased. And two time constants were obtained from the EIS spectra, which also reflected the formation of the passivation film.

The XRD patterns and FE-SEM results showed that the prepared deposits were amorphous. But after a 15 d standard salt spray test, a few pinholes appeared on the deposit and the weight content of phosphorus on the surface of the deposit was higher, which was beneficial to the formation of the passivation film, than it was before the standard salt spray test, while the nickel content was lower because the dissolved weight of nickel was greater than that of phosphorus. The results from potentio-dynamic scan and EIS showed that passivation film formed on the Ni-P deposit after immersion in 3.5% NaCl solutions and decreased the corrosion rate of Ni-P samples.

References

David, J., and D. B. Brown, 1997. 'The Effect of Ozone on the Corrosion Behavior of Ni-Cr-Mo Alloys in Artificial Seawater' in Electrochemical Methods in Corrosion. *Research*

and Application, Elsener, B. ed., Trans. Tech. Publications, Switzerland, 37pp.

Diegle, R.B, N. R. Sorensen, C. R. Claytan, and M.A. Helfand, 1988. An XPS Investigation into the Passivaty of an Amorphous Ni-2OP Alloy. *J. Electrochem. Soc.*, **5** (135): 5-9.

Donald, E, S. Storjonann, and .J.Wiberg, 1984. Methods and Apparatus for Maintaining Electroless Plating Solution, US005484626A.

Feldstein, N., and S. L. Thomas, 1980. Cobalt as a Stablizer in Electroless Plating Formulations, US005480477A.

Hajdu, J, 1996. Electroless plating: the past is prologue. *Plat. Surf. Finish.*, **83** (9): 29-33.

Han, K. P., Y. Wu, M. Zhang, and J. H. Wang, 1996. A Super High Speed Electroless Nickel Plating Proces. *Trans. IMF*, **74** (3): 91-94.

Hou, X. M., 2000. Anodic Behavior and Polarization of Electroless Ni-P Amorphous Alloy Coating. *J. Anhui Inst. Archit.*, **8** (2): 73-77 (in Chinese).

Lin, K. L., and P. J. Lai, 1989. The crystallization of an electroless Ni-P depoait. *J. Electrochem. Soc*., **5** (136): 3803-3807.

Mallory, G. O., and V. A. Lioyd, 1985. Kinetics of Electroless Nickel Coatingion with Sodium Hypophosphite -an Empirical Rate law, *Plat. Surf. Finish.*, **37** (9): 52-57.

Niu, Zh. B., T. H. Wu, and Z. L. Li, 2003. In situ XRD Investigation on the Crystallization Behaviors of Electroless High-Phosphorous Ni-P Alloys. *Acta Phys.-Chim. Sin.*, **19** (8): 705-708.

Sun, D. B., D. J. Yang, and R. Zh. Zhu, 1992. Repossivation Behavior of Amorphous Ni～P Alloy. *J. Univ. Sci. Technol. Beijing*, **11** (2): 239-243 (in Chinese)

Taloat, A., E. Mallah, M. H. Hassib, I. A. Mekhaeel, and M. Younan, 1993. Autoanalytic (Electroless) Coatingion of Nickel (Phosphorus) Boron Allors: Part Ⅱ/Coating Properties, *Metal Finishing*, **3** (8): 23-28.

Xu, J. Zh., and B. M. Wei, 2000. The Corrosion Behavior of Electroless Ni-Cu-P Alloy in Weak Acid Medium Full of CO_2 at High Temperature by XPS. *Corr. Sci. and Prot. Tech.*, **12** (2): 72-75 (in Chinese).

Yang, Y. G., D.B. Sun, and D. J. Yang, 2000. Corrosion Resistance of Electroless Ni-Cr-P Plating in NaCI Solution. *Corr. Sci. and Prot. Tech.*, **12** (3): 138-142 (in Chinese).